A major purpose of the Technical Information Center is to provide the broadest dissemination possible of information contained in DOE's Research and Development Reports to business, industry, the academic community, and federal, state and local governments.

Although portions of this report are not reproducible, it is being made available in microfiche to facilitate the availability of those parts of the document which are legible.

LA-UR-86-4362

CONF-8610236--1

Los Alamos National Laboratory is operated by the University of California for the United States Department of Energy under contract W-7405-ENG-36.

MASTER

LA-UR--86-4362

DE87 003761

TITLE: The P/Giacobini-Zinner Magnetotail

AUTHOR(S): J.A. Slavin, E.J. Smith, P.W. Daly, K.R. Flammer, G. Gloeckler, B.A. Goldberg, D.J.McComas, F.L. Scarf and J.L. Steinberg

SUBMITTED TO: Proceedings of the 20th ESLAB Symposium, 27-31 October 1986, Heidelberg, West Germany

DISCLAIMER

Los Alamos Los Alamos National Laboratory
Los Alamos, New Mexico 87545

FORM NO 836 R4
ST NO 2629 5/81

THE P/GIACOBINI-ZINNER MAGNETOTAIL

J. A. Slavin[1], E.J. Smith[1], P.W. Daly[2], K.R. Flammer[3], G. Gloeckler[4], R.A. Goldberg[1], D.J. McComas[5], F.L. Scarf[6], and J.L. Steinberg[7]

Abstract

On September 11, 1985 the International Cometary Explorer passed behind Comet Giacobini-Zinner with a closest approach distance of 7800 km. In agreement with Alfven's interplanetary magnetic field line draping model of cometary type I tails, a well defined 1 x 10^4 km diameter magnetotail was observed downstream of the inner coma. This study uses the ICE magnetic field, plasma electron, plasma wave, and energetic ion observations to investigate the structure and stability of the Giacobini-Zinner magnetic tail. Emphasis is placed on the identification of differences and similarities between cometary and planetary magnetotails. Finally, the ICE magnetotail observations are discussed in relation to the global solar wind interaction with P/Giacobini-Zinner.

Keywords: Giacobini-Zinner, cometary magnetotail, current layers, reconnection.

1. Introduction

The International Cometary Explorer (ICE) Mission to P/Giacobini-Zinner (G-Z) has returned the first in situ measurements in a cometary magnetotail (ref. 1,2). Combined with the upstream solar wind, ionosheath, and ionospheric observations at P/Halley taken by Sakigake, Suisei, Vega 1/2, and Giotto, the 1985-6 comet missions have provided a very comprehensive first look at the solar wind interaction with comets. This paper reports the results of a G-Z magnetotail study utilizing magnetic field (ref. 3), electron plasma (ref. 4, 5), plasma wave (ref. 6), and energetic particle (7,8) observations recorded by ICE on September 11, 1985. The findings will be discussed with an emphasis on identifying major differences between the solar wind interaction with comets as opposed to planetary magnetic fields and ionospheres.

1) Jet Propulsion Laboratory, Pasadena, California, USA
2) Max-Planck Institut fur Aeronomie, Katlenburg-Lindau, FRG
3) University of California at San Diego, La Jolla, California, USA
4) University of Maryland, College Park, Maryland, USA
5) Los Alamos National Laboratory, Los Alamos, New Mexico, USA
6) TRW Space and Technology Group Redondo Beach, California, USA
7) Observatorie de Paris, 92195 Meudon, Principal Cedex, France

2. Tail Morphology

The interplanetary magnetic field line draping model of cometary type I, or ion, tails advanced by Alfven (ref. 9) was dramatically confirmed by the ICE magnetic field observations as shown in the top panel of Figure 1 (ref. 3, 10). The position of the ICE spacecraft and six second averages of the magnetic field have been projected into the solar wind aberrated cometocentric solar ecliptic coordinate system where X' is antiparallel to the inferred solar wind velocity vector in the comet rest frame, Y' is parallel to the ecliptic plane and positive in a retrograde sense, and Z' completes the right-handed system (ref. 11). As shown, the spacecraft observed turbulent, weakly draped magnetic fields in the ionosheath. Near Z' ~-5 x 10^3 km, the magnetic field rapidly increased in magnitude and rotated to a more strongly draped configuration as ICE passed behind the inner coma. Shortly before closest approach, the magnetic field intensity dropped from a peak value of ~ 60 nT to 5-10 nT and its direction changed to an orientation transverse to the X' axis. The outbound magnetic field observations are very similar, but with the polarity reversed. Initial studies of these observations (ref. 10 13) have interpreted them as indicating the presence of a draped-field magnetotail of quasi-cylindrical cross section composed of two magnetic lobe regions separated by a diamagnetic plasma sheet.

The bottom panel of Figure 1 displays a schematic of the magnetic field draping pattern corresponding to the ICE magnetic field observations. The current sheet forming the outer boundary of the tail has been modeled as a parabola based on the orientations of the normal vectors derived from minimum variance analyses (ref. 10). The model tail surface intersects the X' axis at a subsolar distance of 730 km from the nucleus. The outer boundary of the lobes should map to the top of the region of strong field line draping upstream of the dayside cometary "obstacle". At Halley, the magnetic field observations (ref. 14) showed a rapid increase in magnetic field strength at a distance upstream of the nucleus that corresponded approximately to the "collisionopause" (ref. 15) where the mean free path for collisions between ionosheath ions and the outflowing cometary neutrals becomes equal to the distance to the nucleus. Inside of this distance a strong slowing of the ionosheath flow was observed (ref. 15).

Radial density profiles for H_2O and electron density in a spherically symmetric atmospheric model of Giacobini-Zinner (ref. 14, M. L. Marconi, private communication, 1986) are displayed in Figure

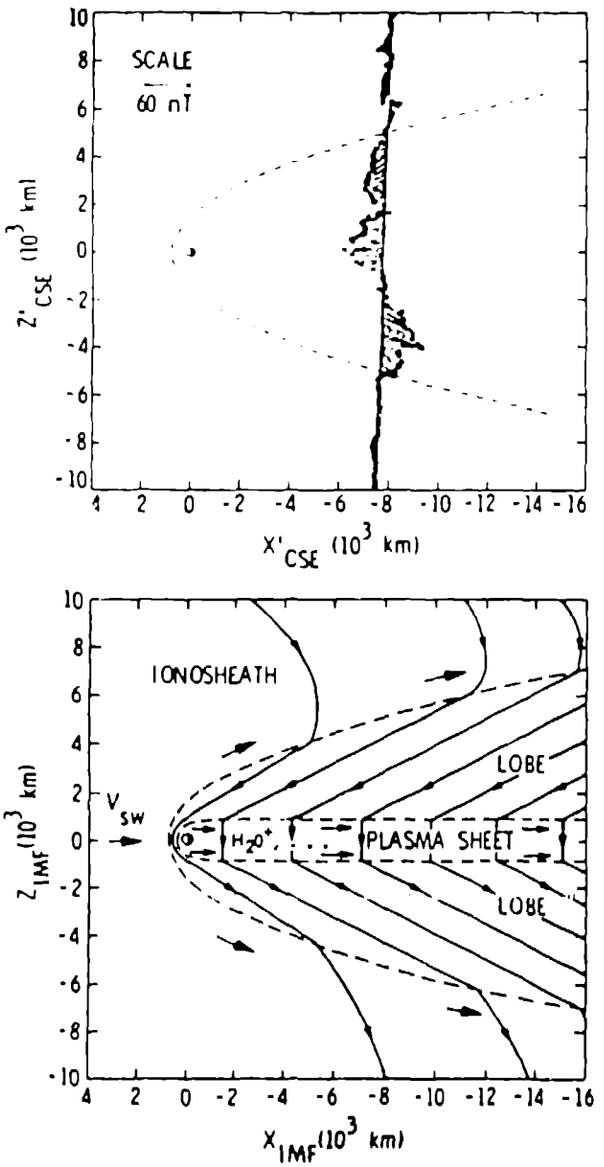

Figure 1. In the top panel, the ICE magnetic field measurements around closest approach to Giacobini-Zinner have been projected into the Z'- X' plane and a parabola fit to the boundary crossings. A schematic diagram of the main cometary magnetotail regions in the plane of the IMF is presented in the bottom panel.

2. The collisional cross sections for H, H_2O, and their ions are poorly known (e.g., ref. 17). However, assuming values of $\sigma \sim 2 \times 10^{-15}$ and 1.5×10^{-15} cm^2, for $H^+ - H_2O$ and $H_2O^+ - H_2O$, respectively, mean free paths for these ionosheath ions have been graphed in Figure 2. The collisionopause occurs at a radial distance from the nucleus of 1-7 $\times 10^3$ km as can be seen from the mean free path profiles. Given the uncertainties in the extrapolated tail surface model, the factor of ~ 2 agreement between the calculated top of the magnetic barrier, R_c, and the extrapolated ICE magnetotail surface is reasonably good.

The lobe-plasma sheet interface is believed to map forward to the discontinuity separating the magnetic barrier from the outflowing cometary iono-

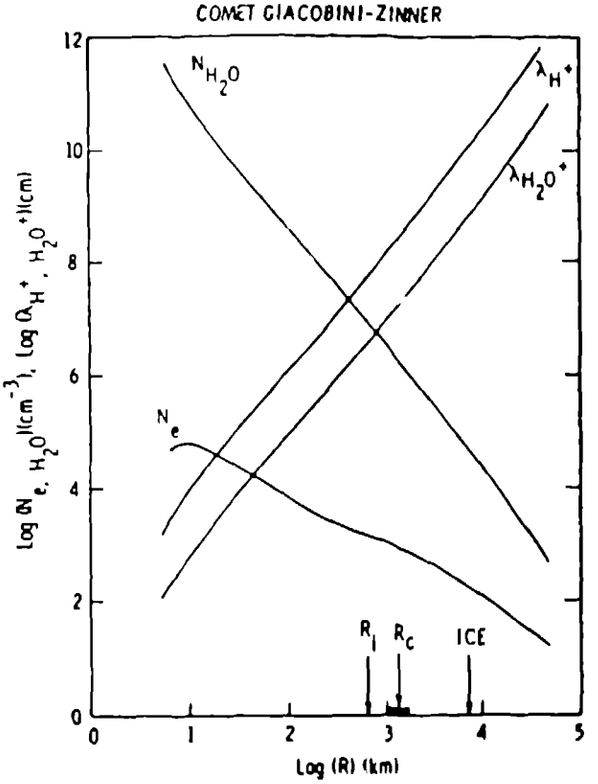

Figure 2. Radial profiles of H_2O and electron density from a spherically symmetric model of the G-Z coma (ref. 16) are presented and used in the calculation of mean-free paths for incident H^+ and H_2O^+ from the ionosheath. Arrows indicate the estimated distances of the subsolar ionopause, R_I, the collisionopause, R_c, and ICE closest approach.

sphere. The presence of the barrier blocks the sunward motion of cometary ions and channels them downstream to form the plasma sheet between the two magnetic lobes (ref. 18, 19) as shown in the bottom panel of Figure 1. The distance to the contact discontinuity, or ionopause, is the point where the external pressure balances the outward pressure of the cometary ionosphere and the collisionally coupled neutrals (i.e., at G-Z the ion-neutral decoupling distance is ~ 2 x 10^3 km). The distance to the subsolar ionopause, R_I, calculated from balancing magnetic tension in the magnetic barrier against the ion-neutral frictional force (ref. 20) yields a value of ~ 6 x 10^2 km (ref. 17) as indicated at the bottom of Figure 2.

The ICE magnetic field and plasma electron observations are plotted in Figure 3. The magnetic field shows very sharp inbound and outbound tail boundaries with rapid increases in $|B_x|$ and $B^2/8\pi$ over the ionosheath values (ref. 10). By comparison, the signatures in the plasma electron measurements were more gradual and corresponded to decreases in temperature and increases in density (ref. 13). The plasma bulk speeds in the tail were less than 30 km/s and too slow to be reliably determined from the electron plasma analyzer measurements (ref. 4). In addition, only the radio experiment's thermal noise spectroscopy measurements of electron density and temperature were able to obtain accurate values in the very cold central plasma sheet (ref. 5). In the absence of low energy ion mea-

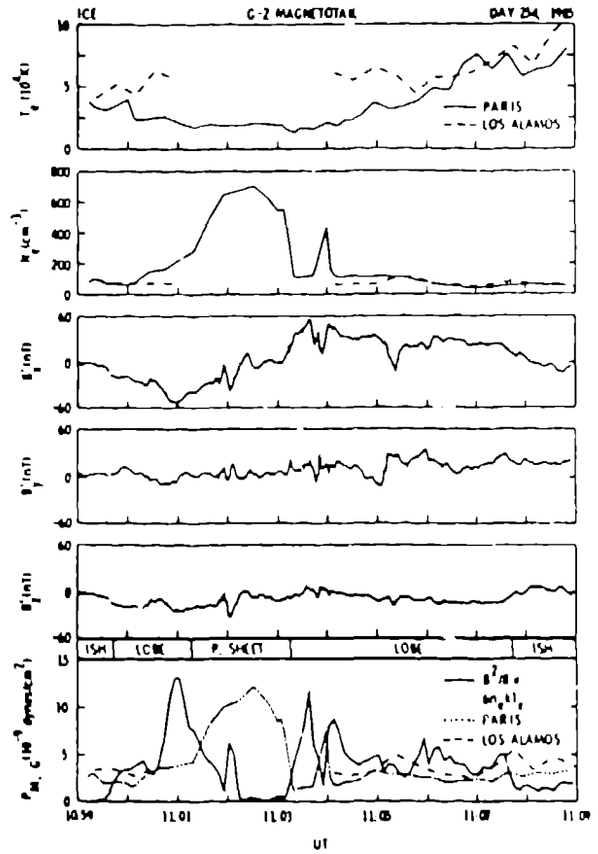

Figure 3. ICE magnetotail observations taken with the JPL vector helium magnetometer (ref. 3), the LANL electron plasma analyzer (ref.4), and the Paris Observatory radio experiment (ref.5) are displayed.

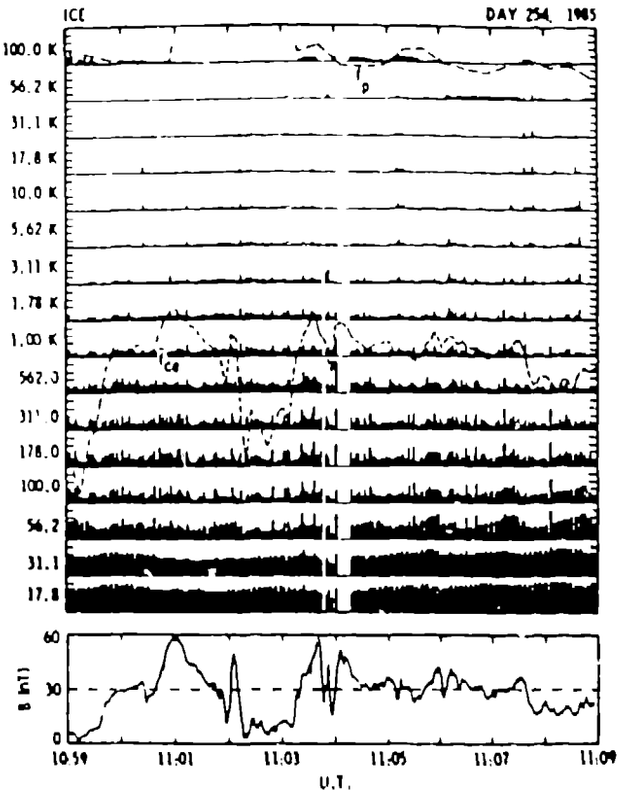

Figure 4. ICE plasma wave electric field amplitudes in the magnetotail are displayed along with the calculated plasma frequency, f_p, and electron cyclotron frequency, f_{ce}.

surements, the total thermal plasma pressure has been estimated by assuming a single T_i/T_e ratio of 5 which brings the plasma sheet and lobe pressures into approximate balance. Given the expected variations in the flow speed at the point of ion pickup, the ratio of T_i/T_e should be a function of position across the tail (ref. 13). However, even with this limitation Figure 3 still shows clearly the anti-correlation between magnetic and thermal pressure. The overall appearance of the G-Z tail is very similar to planetary magnetotails at Earth and Venus (e.g., ref. 21) except for the factor of two variation in magnetic field intensity across the lobe regions and the extreme coolness of the plasma sheet.

Figure 4 shows the electric field plasma wave amplitudes detected as ICE made its closest approach to Comet Giacobini-Zinner. For comparison, the magnetic field magnitude is plotted in the bottom panel. For each E-field channel the amplitude variation from panel bottom to top is approximately a factor of 100,000. Dashed curves display the electron plasma frequency, f_p, and the electron cyclotron frequency, f_{ce}, calculated from the plasma density and magnetic field magnitude measurements. Although intense plasma waves with amplitudes that nearly caused saturation of the instrument were detected over a large region outside of the tail (ref. 6), it can be seen that only moderate wave levels were detected in the magnetotail. The isolated sporadic low frequency impulses represent dust impacts on the spacecraft (ref. 22), while the steady low frequency, $f < 3$ kHz, waves are probably ion acoustic oscillations (whistlers are ruled out because they normally would have a cutoff in the range $f_{ce}/4$ to $f_{ce}/2$). The enhancements in the upper channels are clearly related to electron plasma oscillations which follow the plasma density variations in Figure 3 and the mid-frequency bursts are broadband turbulence similar to that detected at the Earth's plasma sheet.

Energetic cometary ions with $E > 65$ keV (for water group ions) were detected from $\sim 2 \times 10^6$ km before closest approach to $\sim 5 \times 10^6$ km afterwards (ref. 7, 8, 23). Upstream of the bow shock, the ions are observed flowing generally in the direction of the solar wind, but the intensities are strongly correlated with the angle the IMF direction makes to the solar wind velocity vector, as expected for newly created ions being accelerated by the $-\underline{V}\times\underline{B}$ motional electric field. Behind the bow shock, the direction of the ions changes (ref. 24, 25) as the solar wind is deflected around the cometary obstacle. The densities of these heavy cometary ions increase from $\sim 10^{-2}$ cm^{-3} at a distance of 1×10^5 km to $\sim 10^{-1}$ km at 5×10^4 km (ref. 26). Within $\sim 5 \times 10^4$ km of closest approach, finite gyroradius effects caused by the energetic ions encountering the strong tail magnetic fields produce a gradual decrease in energetic ion intensity as displayed in Figure 5. The rotation of the anisotropy vector, not shown, has been used to successfully infer the orientation of the cross-tail current layer (ref. 27).

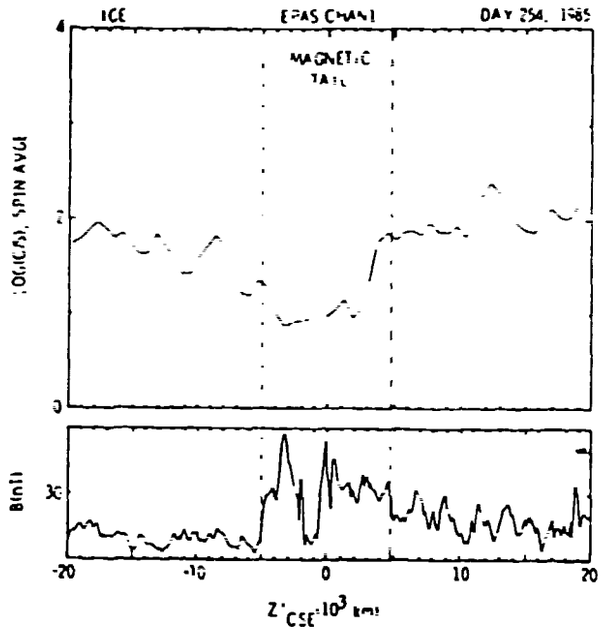

Figure 5. The ICE energetic particle anisotropy spectrometer (EPAS) channel 1 (i.e., 65-95 keV for 0°) counting rate near closest approach is plotted versus Z'.

5. Magnetopause Current Layer

The ICE magnetic field and plasma analyzer electron measurements across the inbound magnetopause are plotted on an expanded time scale in Figure 6. The outer boundary of the tail is marked by a rapid rise in magnetic field intensity, a rotation toward a more tail-like orientation, a decrease in electron temperature, and an increase in density. As shown in the bottom panel, the assumption of $T_i/T_e \sim 5$, which results in approximate pressure balance at the lobe-plasma sheet boundary, also produces equality between the ionosheath thermal pressure and the lobe magnetic field pressure. The total pressure across the magnetopause, however, cannot be brought into balance with a single T_i/T_e. Accordingly, the magnetopause must also represent a discontinuity in ion temperature as already incorporated in some cometary tail models (ref. 12, 13). Such a variation is expected because the flux tubes within the magnetotail would not be there had they not been mass loaded by their interaction with the coma and slowed to a much greater degree than the flux tubes in the adjacent ionosheath. This being the case, the thermal speeds of the picked up cometary ions in the lobes will be correspondingly less.

In Figure 7, the results of a minimum variance analysis of the inbound magnetopause measurements are presented. The surface normal was well determined, the magnetic field executed a rotation in the maximum - intermediate variance plane, and the normal field component is small and comparable in magnitude to the uncertainty in that component associated with the eigenvector determination. Hence, it can be concluded that, locally, the structure of the magnetopause at the time of the ICE crossing appears to be consistent with that of a tangential discontinuity.

The direction of the magnetopause normal in Figure 7 indicates a large flaring angle of $\alpha = 31°$ (i.e., the complement of the angle the normal makes to the X' axis). A similar flaring angle was also inferred

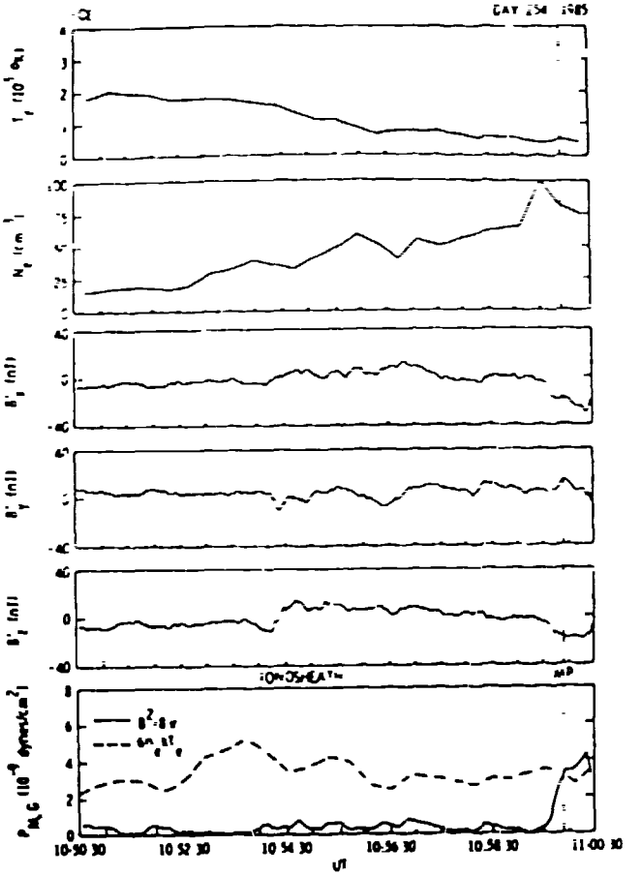

Figure 6. High resolution JPL magnetic field and LANL electron observations across the inbound tail boundary, or "magnetopause", are displayed.

for the outbound magnetopause (not shown). These flaring angles are larger than those observed a comparable number of solar wind stand-off distances down the Earth's magnetotail (ref. 28). In the case of a magnetosphere, there is no significant mass loading due to the high altitude at which the magnetopause is located. The solar wind is, therefore, able to be re-accelerated up to solar wind-like speeds by the time a fluid parcel passes the dawn-dusk terminator plane. Accordingly, the ram pressure of the flow, $\rho V^2 \sin^2 \alpha$, is able to generate large external pressures for very small flaring angles. In the case of comets, there is a conversion of upstream ram pressure into thermal pressure as the pick-up process creates very hot ions at the expense of flow speed. As a result, the cometary magnetopause flares to relatively large angles before the ram plus static pressures balance the internal pressure of the tail. Much farther downstream, the ionosheath flow eventually reaches high speeds and the flaring angle decreases in agreement with ground-based ion tail imaging (ref. 29).

The high resolution magnetic field measurements in Figure 7 show the G-Z magnetopause to have been crossed in approximately 5 sec, or ~ 100 km. Studies at the Earth have found the width of the magnetopause current layer to be 1 - 10 proton gyroradii (ref. 29). In the case of a comet, it might be expected that the heavy ions in the ionosheath, which account for most of the external pressure (ref. 12, 13), would be important in determining the thickness of the outer boundary of the tail. However, the H_2O^+ gyroradius is given by

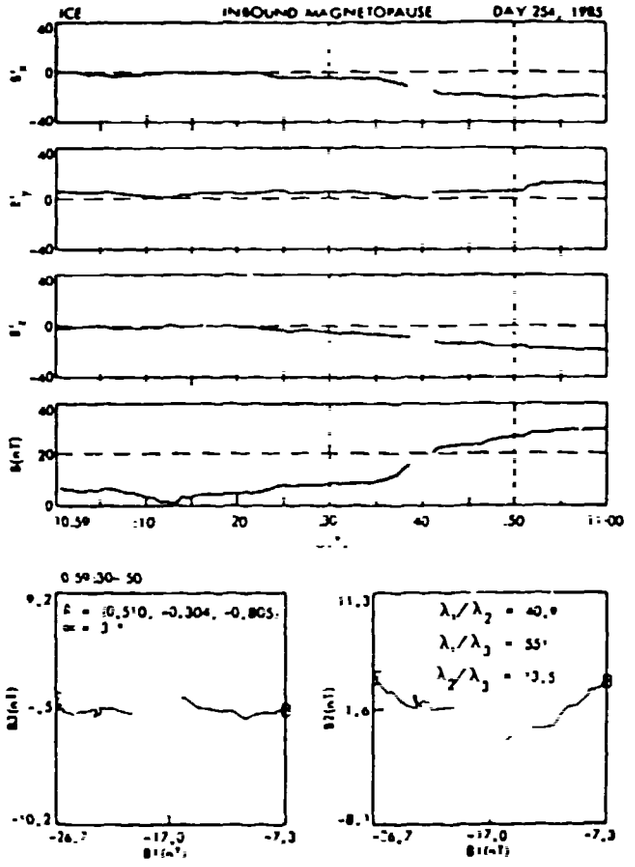

Figure 7. ICE magnetic field observations across the inbound "magnetopause" are plotted in minimum variance coordinates along with the eigenvalue ratios, normal direction, and flaring angle.

$$R_g(km) = 3 \times 10^{-4} (T_i(°K)/B^2(G))^{1/2} \quad (1)$$

and, if the 10^6 °K pickup ion temperature adjacent to the tail boundary inferred from modeling studies (ref. 13) and B = 30 nT is used, then the H_2O^+ ion gyroradius is 10^3 km as compared with the observed current layer thickness of 10^2 km. Accordingly, the thickness of the cometary magnetopause does not appear to be determined by the heavy pickup ions. Solar wind H^+ ions in the ioncsheath with temperatures of 10^5 to 10^6 °K have gyroradii of ~ 20 to 50 km which would be consistent with the terrestrial observations of 1-10 R_g wide magnetopause current layers.

4. Cross-Tail Current Layer

The ICE magnetic field observations across the G-Z plasma sheet are plotted on an expanded time scale in Figure 8. As discussed earlier, the plasma sheet - lobe interface is expected to map forward to the dayside ionopause with the plasma observed at ICE being ionospheric ions which have been deflected tailward by the presence of the magnetic barrier (ref. 18). The Giotto magnetic field observations at Halley (ref. 14) showed the dayside ionopause of that comet to be a relatively thin, < 10^2 km, discontinuity surface with little or no interplanetary magnetic field penetration into the ionosphere. The ICE plasma and magnetic field measurements in Figure 8, in contrast, show a very broad, ~ 10^3 km, boundaries between the high beta plasma sheet and the magnetic lobes. In addition, the high ion temperatures required to balance

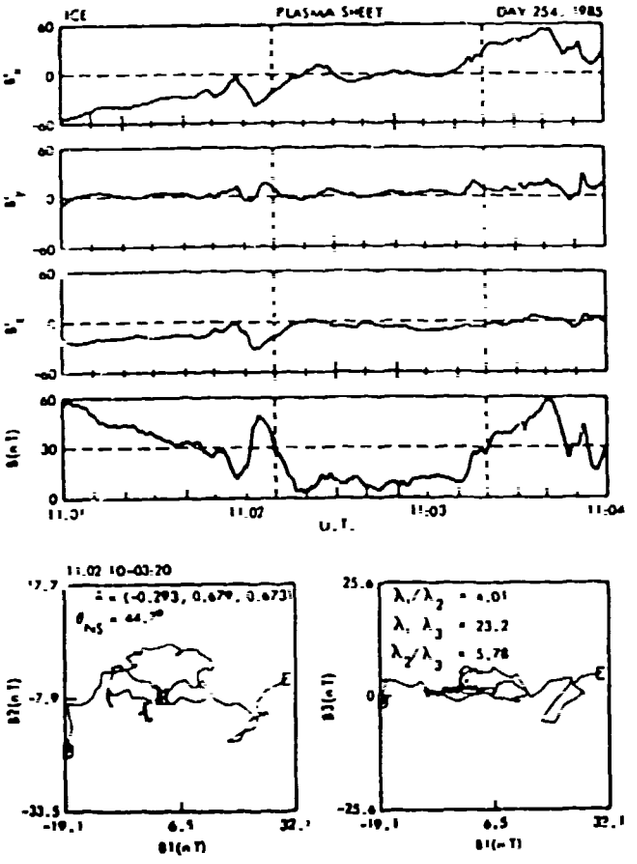

Figure 8. ICE magnetic field observations in the cross-tail current layer are displayed in minimum variance coordinates along with the eigenvalue ratios, normal direction, and "neutral sheet" inclination angle.

pressure between the lobes and plasma sheet (i.e., $T_i \sim 10^5$ °K in Figure 3) are consistent with their being picked up by slow, ~ 10 km/s, flows in the vicinity of the ionopause (ref. 13). Accordingly, the ICE observations suggest that the G-Z plasma sheet may be composed of both cold ionospheric and hotter pick-up ions which have penetrated the ionopause.

The stability of the cometary ionopause is also important for consideration of interplanetary magnetic field penetration into the ionosphere. It has been shown using linear MHD treatments that this surface is instrinsically unstable to several modes: flute, Kelvin-Helmholtz, and drag. However, for the conditions that prevail at the ionopause, the Kelvin-Helmholtz instability, driven by the velocity shear, dominates (ref. 33). Furthermore, the existing solar wind conditions determine the size of this velocity shear, and for small shears, < 2 km/s, the growth time of the instability is much larger than the convections time. Hence, for some solar wind conditions the instability does not develop and the surface is well defined. Accordingly, additional studies of solar wind conditions during the Giacobini-Zinner encounter may be necessary to resolve the stability question and determine the origin of the 5-10 nT magnetic fields observed in the plasma sheet.

A minimum variance analysis has been carried out on the magnetic field across the central plasma sheet,

~ 11:02:10-11:03:20, with the results displayed at the bottom of Figure 8. The magnetic field in the maximum-intermediate variance plane exhibits a net rotation from the orientation of the inbound lobe, $B1<0$, to the outbound lobe, $B1>0$. The minimum variance direction for this simple draping pattern indicates an inclination in the Y'- Z' plane, $\theta_{nn'}$, of the current layer to the ecliptic of 44.7°. This result is in excellent agreement with the determinations of the current sheet orientation by other methods (ref. 11, 13, 27). The non-zero X' normal component is indicative of the large degree of flaring in the G-Z near-tail.

The cross-tail current layer at Giacobini-Zinner is not highly localized as in planetary magnetotails, but rather it extends across the full width of the plasma sheet. If that width is judged on the basis of the points where the thermal plasma pressure equals the magnetic field pressure, and the inclination of the current sheet and the ICE trajectory are taken into account, then a current layer thickness of 1.5×10^3 km is found. If the current is to be carried by the heavy ions, then this width must be comparable to or greater than the H_2O^+ gyroradius. Assuming $T_i/T_e \sim 5$, $T_e \sim 15{,}000$ °K, and $B \sim 8$ nT, (1) yields $R_g \sim 1 \times 10^3$ km. Accordingly, the thickness of the cometary crosstail current sheet is comparable to 1-2 ion gyroradii, or similar to some of the thinnest neutral sheets observed in the Earth's magnetotail (ref.31).

The nature and stability of the cross-tail current layer are fundamental questions for all magnetotails. For intrinsic field magnetospheres, the cross-tail current is carried by the plasma sheet ions, primarily H^+ from the solar wind, and can be as thin as a few ion gyroradii. In the reconnection models of magnetospheric dynamics, a "substorm" is initiated when thinning of the plasma sheet due to magnetic flux addition to the lobes has reduced the current sheet width to the point where the ions become unmagnetized. An exponential growth in the tearing mode is then thought to occur (ref. 32) and to result in the rapid transfer of magnetic energy into plasma heating and high speed flows as commonly observed during substorms.

Observations from the Earth of abrupt variations in the appearance of cometary rays and the central ion tail have led to the hypothesis of reconnection both in the cross-tail current layer, and following interplanetary sector boundary reversals, at the dayside ionopause (ref. 33). The results of this study indicate that, assuming a H_2O^+ dominated plasma sheet, the Giacobini-Zinner cross-tail current sheet is only 1 - 2 ion gyroradii thick. Therefore, it is potentially unstable to the tearing mode instability, if initiated by sufficiently large amplitude perturbations or driving forces and allowed sufficient growth time without being stabalized by the lighter plasma sheet ion species and electrons. However, it must be noted that none of the dissipation signatures, such as energetic particle acceleration, high speed flows, $+/- B_n$ magnetic fields, and enhanced plasma wave emissions, usually associated with tail reconnection at the Earth were observed during the brief ICE passage through the G-Z magnetotail.

5. Summary

The ICE measurements at P/Giacobini-Zinner show the presence of a well defined 1×10^4 km diameter magnetotail consisting of two magnetic lobes separated by a 1.5×10^3 km wide plasma sheet. In terms of the global interaction, the high beta plasma sheet region is expected to map back to a $\sim 6 \times 10^2$ km radius ionopause sunward of the nucleus. The outer boundary of the lobe is the downstream extension of the top of the magnetic barrier which may correspond to the collisionopause (i.e., $R_c \sim 10^3$ km). The ICE observations show this boundary to be a thin magnetopause-like current layer. Minimum variance analysis of the cometary magnetopause yields a well determined minimum variance direction and a small normal field component consistent with it being, locally, a tangential discontinuity. The thickness of the cometary magnetopause is much less than a heavy ion gyroradius, i.e., comparable to several H^+ gyroradii. The orientation of the magnetopause normal indicates the presence of considerable flaring, $\alpha \sim 31°$, and suggests an approximately parabolic shape for the near-tail surface. The cross-tail current sheet occupies nearly the full width of the plasma sheet, but is only one or two H_2O^+ gyroradii thick. The thinness of the cross-tail current sheet in terms of the gyroradius of the heavy ions raises the possibility of marginal stability against ion tearing mode reconnection. However, ICE did not observe any of the typical magnetospheric signatures of reconnection. Rather, a simple draping pattern was observed in excellent agreement with Alfven's original cometary magnetic tail model.

6. Acknowledgements

The research done at Los Alamos National Laboratory was performed under the auspices of the United States Department of Energy with support from NASA under S-04039-D. The research carried out at the Jet Propulsion Laboratory of the California Institute of Technology was performed under contract to the National Aeronautics and Space Administration.

7. References

1. Science, 1986, 232, 353-385.
2. Geophys. Res. Lett., 1986, 13, 237-99.
3. Smith, E.J., et al., 1986, International Cometary Explorer encounter with Giacobini-Zinner: Magnetic field observations, Science, 232, 382-5.
4. Bame, S.J., et al., 1986, Comet Giacobini-Zinner: Plasma description, Science, 232, 356-61.
5. Meyer-Vernet, N., et al., 1986, Plasma diagnosis from thermal noise and limits on dust flux or mass in Comet Giacobini-Zinner, Science, 232, 370-3.
6. Scarf, F.L., et al., 1986, Plasma wave observations at Comet Giacobini-Zinner, Science, 232, 382-4.
7. Hynds, R.J., et al., 1986, Observations of energetic ions from Comet Giacobini-Zinner, Science, 232, 361-5.
8. Ipavich, F.M., et al., 1986, Comet Giacobini-Zinner: In situ observations of energetic heavy ions, Science, 232, 366-9.
9. Alfven, H., 1957, On the theory of comet tails, Tellus, 9, 92-6.
10. Slavin, J.A., et al., 1986, Giacobini-Zinner magnetotail: ICE magnetic field observations, Geophys. Res. Lett., 13, 283-6.
11. Slavin, J.A., et al., 1986, The structure of a cometary type I tail: Ground-based and ICE observations of P/Giacobini-Zinner, Geophys. Res. Lett., 13, 1085-8.
12. Siscoe, G.L., et al., 1986, Statics and dynamics

of the Giacobini-Zinner magnetic tail, Geophys. Res. Lett., 13, 287-90.
13. McComas, D.J., et al., 1986, The Giacobini-Zinner magnetotail: Tail configuration and current sheet, J. Geophys. Res., in press.
14. Neubauer, F.M., et al., 1986, First results from the Giotto magnetometer experiment at Comet Halley, Nature, 321, 352-5.
15. Mendis, D.A., et al., 1986, On the global nature of the solar wind interaction with Comet Halley, unpublished manuscript.
16. Marconi, M.L., and Mendis, D.A., 1986, The electron density and temperature in the tail of Comet Giacobini-Zinner, Geophys. Res. Lett., 13, 405-6.
17. Mendis, D.A., et al., 1986, Comet-solar wind interaction: Dynamical length scales and models, Geophys. Res. Lett., 13, 239-42.
18. Wallis, M.K., and Dryer, M., 1976, Sun and comets as sources in an external flow, Ap. J., 205, 895-9.
19. Houpis, H.L.F., and Mendis, D.A., 1981, On the development and global oscillations of cometary ionospheres, Ap. J., 243, 1088-92.
20. Ip, W.-H., and Axford, W.I., 1982, Theories of physical processes in cometary coma and tails, Comets, ed. L.L. Wilkening, 588-634.
21. Slavin, J.A., et al., 1984, A comparative study of distant magnetotail structure at Venus and Earth, Geophys. Res. Lett., 11, 1074-7.
22. Gurnett, D.A., et al., 1986, Dust particles detected near Giacobini-Zinner by the ICE plasma wave instrument, Geophys. Res. Lett., 13, 291-4.
23. Sanderson, T.R., et al., 1986, The interaction of heavy ions from Comet Giacobini-Zinner with the solar wind, Geophys. Res. Lett., 13, 411-4.
24. Richardson, I.G., et al., 1986, Three dimensional energetic ion bulk flows at Comet Giacobini-Zinner, Geophys. Res. Lett., 13, 415-8.
25. Tranquille, C., et al., 1986, Energetic ion properties near the Giacobini-Zinner, Geophys. Res. Lett., 13, 853-6.
26. Gloeckler, G., et. al., 1986, Cometary pick-up ions observed near Giacobini-Zinner, Geophys. Res. Lett., 13, 251-4.
27. Daly, P.W., et al., 1986, Gyroradius effects on the energetic ions in the tail lobes of Comet Giacobini-Zinner, Geophys. Res. Lett. 13, 419-22.
28. Ershkovich, A.I., et al., 1982, On the flaring of cometary plasma tails, Geophys. Res. Lett., 13, 396-406.
29. Berchem, J., and Russell, C.T., 1982, The thickness of the magnetopause layer: ISEE-1 and -2 Observations, J. Geophys. Res., 87, 2108-14.
30. Ershkovich, A. I., et al., 1986, Stability of the sunlit cometary ionopause, Ap. J., in press.
31. Fairfield, D.H., et al., 1981, Multiple Crossings of a very thin plasma sheet in the Earth's magnetotail, J. Geophys. Res., 86, 11189-200.
32. Schindler, K., 1984, Spontaneous reconnection, Magnetic Reconnection in Space and Laboratory Plasmas ed. E.W. Hones, AGU, Washington, D.C., 9-19.
33. Niedner, M.B., and Brandt, J.C., 1978, Plasma tail disconnection events in comets: Evidence for magnetic field line reconnection at interplanetary sector boundaries, Ap. J., 238, 723-32.